Relative Influence of Accelerometer and Displacement Transducer Signals in Road Roughness Measurements

BOHDAN T. KULAKOWSKI, JOHN J. HENRY, AND JAMES C. WAMBOLD

Highway agencies conduct regular testing programs to monitor road roughness characteristics. Measurement of road roughness does not present an extremely challenging problem conceptually. On the other hand, the cost of the measuring equipment is significant. In this paper, the possibility of evaluating road roughness without an accelerometer is considered. The analysis of the frequency characteristics of displacement transducer and accelerometer signals indicates that the latter signal carries very little additional profile-related information within the frequency range of interest in the measurement of road roughness. The analytical conclusions are confirmed by statistical analysis of actual road roughness data.

Roughness is a property of pavement surface that affects not only ride comfort but also highway safety and vehicle energy consumption. Highway agencies conduct regular testing programs to monitor road roughness characteristics. From a conceptual standpoint, measurement of road roughness does not present an extremely challenging problem. On the other hand, the cost of the measuring equipment is a significant factor in the evaluation of road roughness. The cost of commercially available profilometers ranges from $35,000 to over $250,000. The cost of response-type road roughness meters is significantly lower, but these devices require periodic calibration using profilometers.

The technique most widely employed in the United States for obtaining road profile data is measurement of acceleration and displacement between the test vehicle and the road surface with an inertial profilometer (*1*). High-pass filtering of the accelerometer signal followed by double integration gives a record of the absolute vertical position of the vehicle body. The displacement signal is then subtracted from the integrated accelerometer signal to produce the road profile record, which can be further processed to obtain road roughness measures.

An alternative approach to determining road roughness was proposed by Watugala (*2*). In this method the calculation of the elevation profile is eliminated, and road roughness index values are generated by the quarter-car model using the accelerometer and displacement transducer signals as the inputs. This simplifies somewhat the data processing involved, but the procedure is still relatively complex and costly.

In this paper, the possibility of evaluating road roughness without an accelerometer is considered. The analysis of the frequency characteristics of displacement transducer and accelerometer signals indicates that the latter signal carries very little additional profile-related information within the frequency range of interest in the measurement of road roughness. The analytical conclusions are confirmed by statistical analysis of actual road roughness data.

Pennsylvania Transportation Institute, The Pennsylvania State University, University Park, Pa. 16802.

FREQUENCY ANALYSIS OF THE QUARTER-CAR MODEL

An objective measure of road roughness is based on the dynamic response of the standard quarter-car model, which is shown in Figure 1 (*3*, *4*). The quarter-car dynamics is described by the following equations:

$$M_s\ddot{z}_s + C_s(\dot{z}_s - \dot{z}_u) + K_s(z_s - z_u) = 0 \quad (1)$$

$$M_u\ddot{z}_u - C_s(\dot{z}_s - \dot{z}_u) - K_s(z_s - z_u) = K_t(w - z_u) \quad (2)$$

The road roughness index is expressed as

$$R_{QC} = 1/L \int_0^L (\dot{z}_s - \dot{z}_u)dl \quad (3)$$

The road profile, w, is calculated using the equation

$$w(t) = \int_0^t a(\tau)\, d\tau d\tau - x(t) \quad (4)$$

where both the displacement transducer signal, $x(t)$, and the accelerometer signal, $a(t)$, are recorded by an inertial profilometer.

A transfer function block diagram of the quarter-car model employed in road roughness analysis is shown in Figure 2. Road profile, $W(s)$, is the input signal to the system. The displacement transducer and accelerometer responses to the input are generated through the transfer functions $G_{WH}(s)$ and $G_{WA}(s)$, relating vehicle body displacement to road profile, and body acceleration to road profile, respectively:

$$G_{WH}(s) = \frac{H(s)}{W(s)} \quad (5)$$

and

$$G_{WA}(s) = \frac{A(s)}{W(s)} \quad (6)$$

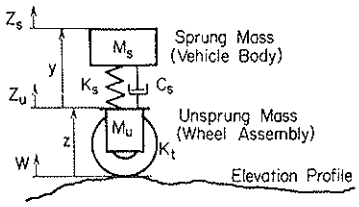

FIGURE 1 Standard quarter-car model.

The relative displacement of the two masses $y(t) = z_s(t) - z_u(t)$ represents the system output. It is related to the displacement transducer and the accelerometer signals through transfer functions $G_{HY}(s)$ and $G_{AY}(s)$ so that

$$Y(s) = G_{HY}(s) \cdot H(s) + G_{AY}(s) + A(s) \tag{7}$$

Using Equations 1 and 2, and noting that

$$H(s) = Z_s(s) - W(s) \tag{8}$$

the detailed expression for $G_{WH}(s)$ in terms of the quarter-car model parameters can be obtained as shown in the Appendix, Equation A1.

Also, taking the Laplace transform of equation 4 we have

$$W(s) = \frac{1}{s^2} A(s) - H(s) \tag{9}$$

and hence the profile-acceleration transfer function can be found as

$$G_{WA}(s) = s^2 [1 + G_{WH}(s)] \tag{10}$$

A detailed expression for $G_{WA}(s)$ is also given in the Appendix, Equation A2.

The other two transfer functions, $G_{HY}(s)$ and $G_{AY}(s)$, can also be expressed in terms of the quarter-car model parameters as shown in the Appendix, Equations A4 and A5. In order to compare the relative effects of the displacement transducer and accelerometer signals on the output signal $Y(s)$, the power spectral densities of the two signals will be considered. First, the power spectral densities of $H(j\omega)$ and $A(j\omega)$ are related to the power spectral density of the input profile signal, $W(j\omega)$, as follows:

$$S_H(j\omega) = S_W(j\omega) \cdot |G_{WH}(j\omega)|^2 \tag{11}$$

and

$$S_A(j\omega) = S_W(j\omega) \cdot |G_{WA}(j\omega)|^2 \tag{12}$$

Next, the power spectral densities of the two components of $Y(j\omega)$, one due to $H(j\omega)$ and the other due to $A(j\omega)$, are expressed as

$$S_{HY}(j\omega) = S_H(j\omega) \cdot |G_{HY}(j\omega)|^2 \tag{13}$$

$$S_{AY}(j\omega) = S_A(j\omega) \cdot |G_{AY}(j\omega)|^2 \tag{14}$$

Combining Equation 11 with Equation 13, and Equation 12 with Equation 14, the expressions for the power spectral densities of the relative body-suspension displacement components caused by the displacement transducer and accelerometer signals, $S_{HY}(j\omega)$ and $S_{AY}(j\omega)$, are found:

$$S_{HY}(j\omega) = S_W(j\omega) |G_{WH}(j\omega)|^2 |G_{HY}(j\omega)|^2 \tag{15}$$

$$S_{AY}(j\omega) = S_W(j\omega) |G_{WA}(j\omega)|^2 |G_{AY}(j\omega)|^2 \tag{16}$$

In order to evaluate the relative effects of the displacement transducer and accelerometer signals on the relative axle-body displacement the function $G(\omega)$ is introduced defined as

$$\sigma(\omega) = \frac{S_{AY}(j\omega)}{S_{HY}(j\omega)} \tag{17}$$

Using equations 15 and 16, $\sigma(\omega)$ can be represented by

$$\sigma(\omega) = \frac{|G_{WA}(j\omega)|^2 |G_{AY}(j\omega)|^2}{|G_{WH}(j\omega)|^2 |G_{HY}(j\omega)|^2} \tag{18}$$

Employing previously derived equations for the transfer functions on the right hand side of Equation 18, $\sigma(\omega)$ can be expressed in terms of the quarter-car parameters, (see Equation A6 in the Appendix).

The plot of $\sigma(\omega)$ is shown in Figure 3. Function $\sigma(\omega)$, introduced above, represents a measure of the relative effect of accelerometer and displacement transducer signals on the axle-body displacement, which, in turn, is used to determine road roughness, Equation 3. It can be observed from Figure 3 that $\sigma(\omega)$ decreases rapidly with the increasing wave number of the road profile. For profile wave number equal to approximately 0.05 cycle/ft the power spectral density of the axle-body displacement related to the accelerometer signal constitutes only about 10 percent of the axle-body displacement component related to the displacement transducer signal. It can therefore be concluded that for wave numbers equal to or greater than approximately 0.05 cycle/ft the dynamics of the axle-body displacement can be accurately represented by the displacement transducer signal only. In a recent study (5) it was found that a subjective measure of road roughness correlates best with the objective measure, represented by the roughness index given by Equation 3, in the range of frequency from 0.125 to 0.63 cycles/ft. It can be seen in Figure 3 that the contribution of the accelerometer signal to the road roughness measure within this frequency range is negligible in comparison with the displacement transducer signal. This analytical conclusion will be verified by statistical analysis of

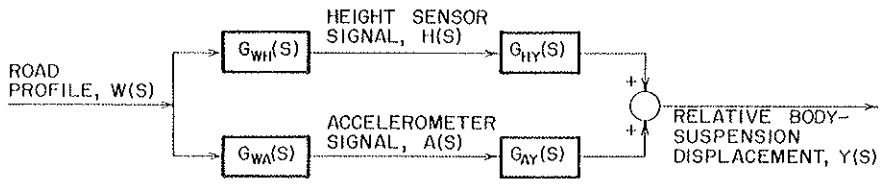

FIGURE 2 Block diagram of the system generating relative axle-body displacement.

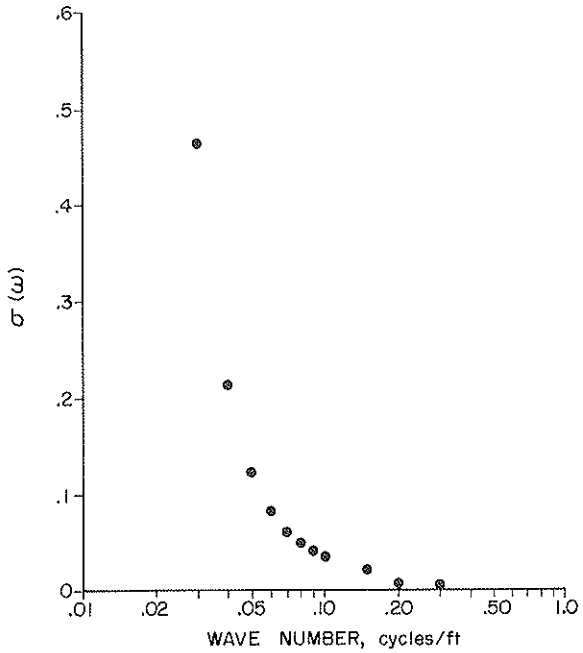

FIGURE 3 Function σ(α) representing relative effect of acceleration and displacement signals on axle-body displacement.

actual road roughness data, which is presented in the next section.

STATISTICAL ANALYSIS

In order to validate the results of the analytical considerations presented in the previous section, a statistical analysis of actual data collected on 15 road sites in Central Pennsylvania was performed. The data were used to calibrate the Pennsylvania DOT's Mays meters (*6*).

First, the roughness index values were calculated for a full quarter-car model using Equation 3. Both the displacement transducer and the accelerometer signals were used as inputs. Next, the accelerometer signal was rejected and only the displacement transducer signal was used as the input to the quarter-car model. This model, with a displacement transducer signal only, will be referred to as the reduced model. The roughness index values were averaged over 0.25-mi intervals. Each road site was 0.5 mi long, and the total number of data points was 30. A regression analysis was performed to yield the following two equations for 25 mph and 40 mph:

$$\hat{R}_{QC} = 3.68 + 1.58R^*_{QC} \text{ at 25 mph} \quad (19)$$

and

$$\hat{R}_{QC} = 5.66 + 1.58R^*_{QC} \text{ at 40 mph} \quad (20)$$

where carets and asterisks are used to denote road roughness index values obtained with the full and reduced models, respectively.

The standard deviation between the road roughness index values obtained from the quarter-car model, R_{QC}, and the values predicted by equations 19 and 20, R_{QC} was found to be 8.51 in/mile and 8.53 in/mile, respectively. The correlation

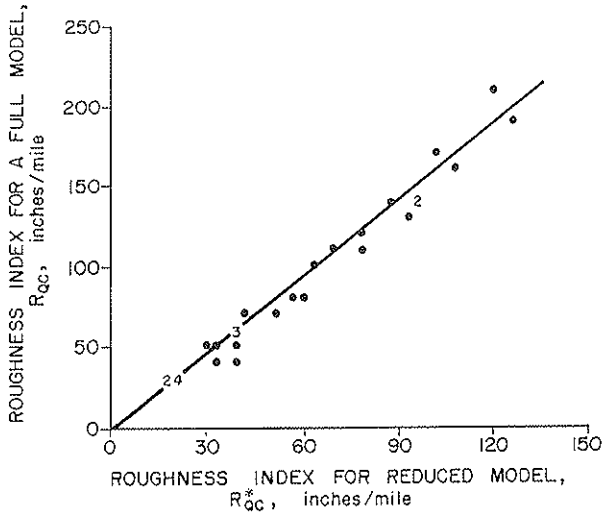

FIGURE 4 Correlation between roughness index values obtained with standard and reduced quarter-car models at 25 mph.

coefficients characterizing the relationship between the complete and the reduced model were 0.99 and 0.98, at 25 mph and 40 mph, respectively. Therefore, it can be concluded that the regression Equations 19 and 20 are statistically meaningful at both speeds. These results are shown in Figures 4 and 5.

In order to further evaluate the usefulness of the reduced model, calibration of the Pennsylvania DOT's Mays meter was performed using the reduced model, and the results were compared with those obtained using a complete quarter-car model (*6*).

The following formulas were obtained with the quarter-car model as the calibration standard:

$$\hat{R}_{QC} = 9.62 + 0.7272R_{MM} \text{ at 25 mph} \quad (21)$$

and

$$\hat{R}_{QC} = 13.1 + 0.664R_{MM} \text{ at 40 mph} \quad (22)$$

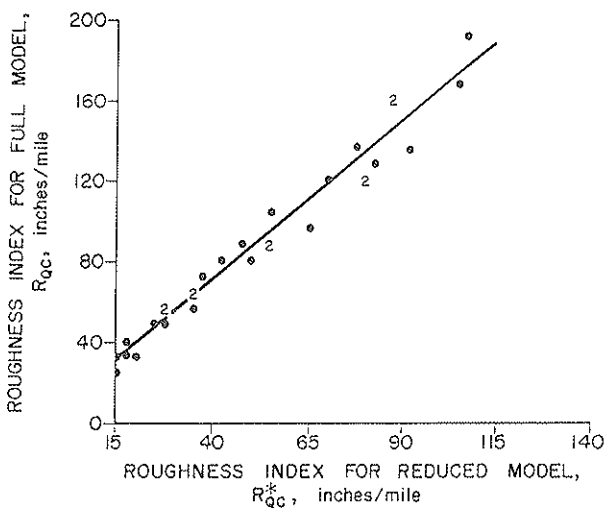

FIGURE 5 Correlation between roughness index values obtained with standard and reduced quarter-car models at 40 mph.

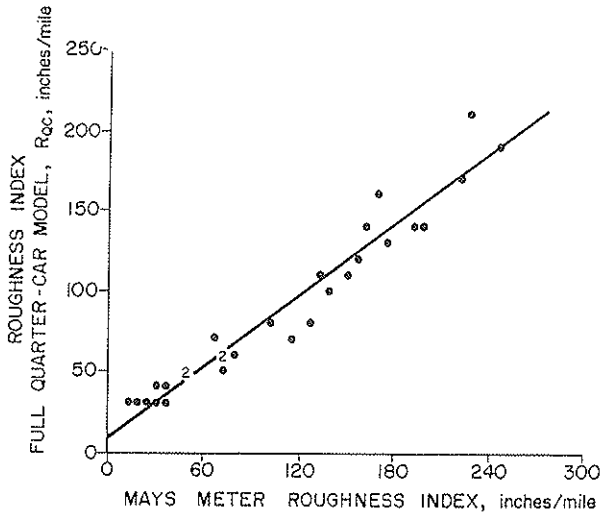

FIGURE 6 Mays meter calibration data using standard quarter-car model at 25 mph.

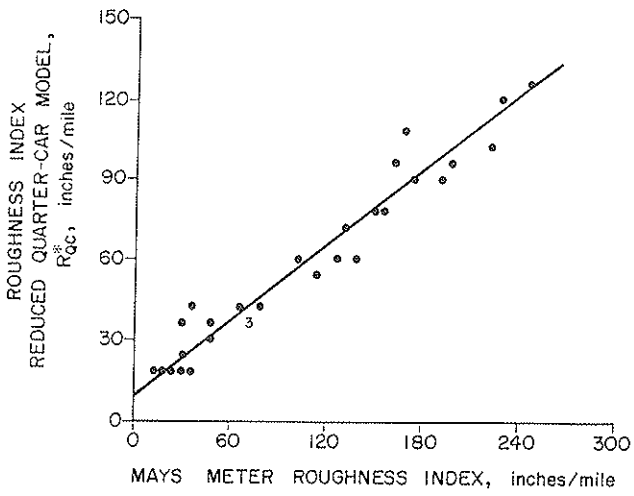

FIGURE 8 Mays meter calibration data using reduced quarter-car model at 25 mph.

The distribution of the experimental data is shown in Figures 6 and 7. Using the reduced quarter-car model as the calibration standard, the following equations were obtained:

$$R^*_{QC} = 9.03 + 0.456R_{MM} \text{ at 25 mph} \quad (23)$$

$$R^*_{QC} = 6.97 + 0.401R_{MM} \text{ at 40 mph} \quad (24)$$

The distribution of the calibration data is shown in Figures 8 and 9. The standard deviations of the measured data from the corresponding regression models were found to be significantly smaller for the reduced model at both speeds: 7.85 versus 12.68 at 25 mph and 9.84 versus 11.53 at 40 mph.

An important aspect of the Mays meter calibration procedure is its sensitivity to speed. In order to investigate the speed effect, the road roughness index values obtained with the reduced model at 25 mph, 35 mph, and 55 mph were correlated, with the quarter-car model at 40 mph used as the reference. The following relations were obtained:

$$\hat{R}_{QC} = 14.0 + 1.29R^*_{QC} \text{ at 25 mph} \quad (25)$$

$$\hat{R}_{QC} = 4.06 + 1.53R^*_{QC} \text{ at 35 mph} \quad (26)$$

$$\hat{R}_{QC} = 11.6 + 1.60R^*_{QC} \text{ at 55 mph} \quad (27)$$

The regression lines described by the above equations, together with the line given by Equation 20 obtained for 40 mph, are shown in Figure 10. It can be seen that the effect of speed is very slight between 35 to 55 mph and that only the results obtained for 25 mph differ significantly.

CONCLUSIONS

The results obtained from both the theoretical and the experimental data analysis indicate that the amount of relevant information carried by the accelerometer signal within the frequency range related to the profile wavelengths that affect road roughness is marginal. The determination of standard

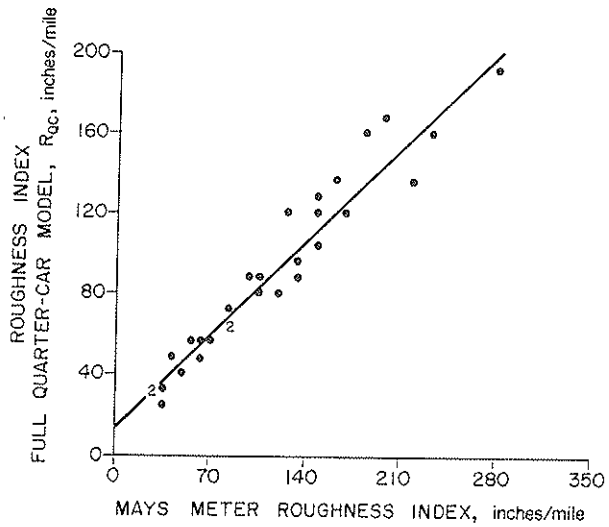

FIGURE 7 Mays meter calibration data using standard quarter-car model at 40 mph.

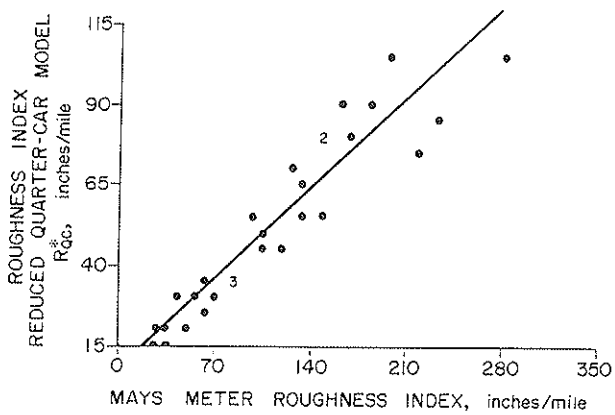

FIGURE 9 Mays meter calibration data using reduced quarter-car model at 40 mph.

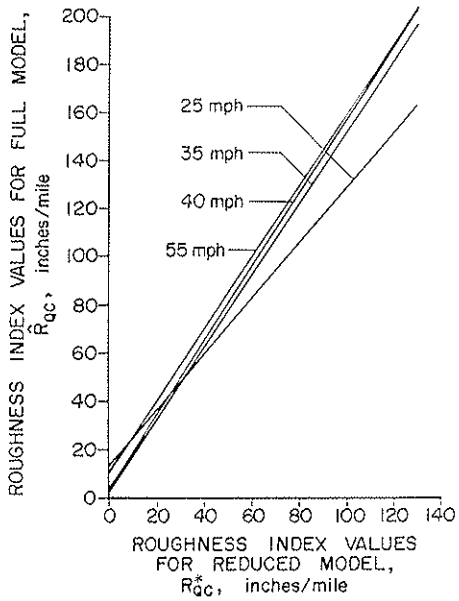

FIGURE 10 Effect of speed on Mays meter calibration lines using reduced quarter-car model.

road roughness measures can, therefore, be accomplished using the body displacement data only. Elimination of the accelerometer will certainly simplify the hardware of the road roughness measurement system; but, more important, it will also allow the software necessary to generate the roughness index to be limited to the processing of the displacement transducer signal. The computational process of calculating the road roughness index without double integrating the accelerometer signal will thus become considerably less expensive.

The results of the analysis presented in this paper, which were obtained with actual displacement and acceleration data, confirm the feasibility of the proposed reduced quarter-car model when used solely for the purpose of roughness index determination.

REFERENCES

1. J. C. Wambold et al. The State of the Art of Measurement and Analysis of Highway Roughness. In *Transportation Research Record 836*, TRB, National Research Council, Washington, D.C., 1981, pp. 21–29.
2. G. K. Watugala. *Determination of Road Roughness from Inertial Profilometer Data*. Ph.D. dissertation, The Pennsylvania State University, 1984.
3. New Standard Practice for Simulating Vehicular Response to Longitudinal Profiles of a Vehicular Traveled Surface. *ASTM Ballot*, September 1985.
4. T. D. Gillespie, M. W. Sayers, and L. Segel. *NCHRP Report 228: Calibration and Correlation of Response-Type Road Roughness Measuring Systems*. TRB, National Research Council, Washington, D.C., 1980.
5. M. S. Janoff et al. *NCHRP Report 1-23: Pavement Roughness and Ride Quality*. TRB, National Research Council, Washington, D.C., 1984.
6. B. T. Kulakowski. *Correlation of Road Roughness Measurements Obtained with the 1962 Chevrolet Impala and with the Standard Quarter-Car Model*. Final Report, Pennsylvania Department of Transportation, July 1985.

APPENDIX

Combining Equations 1 and 2 and taking a Laplace transformation, the transfer function $G_{WH}(s)$ relating the displacement transducer signal to the road profile is obtained:

$$G_{WH}(s) = \frac{s^4 + C_s/M_s + C_s/M_u\, s^3 + K_s/M_s + K_s/M_u + K_t/M_u s^2}{B(s)} \tag{A1}$$

where the polynomial $B(s)$ is

$$B(s) = s^4 + \frac{C_s}{M_s} + \frac{C_s}{M_u} s^3 + \frac{K_s}{M_s} + \frac{K_s}{M_u} + \frac{K_t}{M_u} s^2 + \frac{C_s K_t}{M_s M_u} s + \frac{K_s K_t}{M_s M_u} \tag{A2}$$

Substituting this form into Equation 1 yields the following expression for the transfer function $G_{WA}(s)$:

$$G_{WA}(s) = \frac{C_s K_t/M_s M_u\, s^3 + K_s K_t/M_s M_u\, s^2}{B(s)} \tag{A3}$$

The transfer functions $G_{HY}(s)$ and $G_{AY}(s)$ can also be obtained from the model equations 1 and 2:

$$G_{HY}(s) = \frac{K_t/M_u\, s^2}{B(s)} \tag{A4}$$

$$G_{AY}(s) = -\frac{K_t/M_u}{B(s)} \tag{A5}$$

Letting $s = j\omega$ in Equations A1, A3, A4 and A5 and substituting into Equation 18, the expression for $\sigma(\omega)$ is found as follows:

$$\sigma(\omega) = \frac{(K_s K_t/M_s M_u)^2 + \omega^2 (C_s K_t/M_s M_u)^2}{\omega^4 \left[\left(-\omega^2 + \frac{K_s}{M_s} + \frac{K_s}{M_u} + \frac{K_t}{M_u}\right)^2 + \omega^2 \left(\frac{C_s}{M_s} + \frac{C_s}{M_u}\right)^2\right]} \tag{A6}$$

Publication of this paper sponsored by the Committee on Surface Properties—Vehicle Interaction.